

## Self-healing mechanism of composite coatings obtained by phosphating and silicate sol post-sealing

Bi-lan LIN<sup>1</sup>, Jin-tang LU<sup>2</sup>

1. School of Materials Science and Engineering, Xiamen University of Technology, Xiamen 361021, China;  
2. School of Materials Science and Engineering, South China University of Technology, Guangzhou 510640, China

Received 24 July 2013; accepted 10 October 2013

**Abstract:** Silicate sol post-treatment was applied to form a complete composite coating on the phosphated zinc layer. The chemical compositions of the coatings were investigated using XPS. The coated samples were firstly scratched and then exposed to the neutral salt spray (NSS) chamber for different time. The microstructure and chemical compositions of the scratches were studied using SEM and EDS. And the non-scratched coated samples were compared. The self-healing mechanism of the composite coatings was discussed. The results show that during corrosion, the self-healing ions in composite coatings dissolve, diffuse and transfer to the scratches or the defects, and then recombine with  $Zn^{2+}$  to form insoluble compound, which deposits and covers the exposed zinc. The corrosion products on the scratches contain silicon, phosphorous, oxygen, chloride and zinc, and they are compact, fine, needle and flake, effectively inhibiting the corrosion formation and expansion of the exposed zinc layer. The composite coatings have good self-healing ability.

**Key words:** corrosion; self-healing; phosphate coatings; silicate; zinc

### 1 Introduction

Phosphate conversion coatings (phosphate coatings) have been widely used to improve the corrosion resistance and the painting capacities of the metals. But the corrosion resistance is impaired by the pores in phosphate coatings [1]. If the pores can be eliminated as thoroughly as possible, the corrosion resistance of phosphate coatings can be enhanced greatly. And if the self-healing ability is obtained, phosphate coatings can be as the replacer for chromate conversion coatings which are highly toxic, carcinogenic and contaminative.

Surface activating before phosphating [2,3], improving the phosphating technologies [4,5] and post-sealing treatment after phosphating [6,7] are important measures to enhance the corrosion resistance of phosphate coatings. Post-sealing treatment can effectively eliminate the pores of phosphate coatings. The traditional post-sealing solution is chromate. Olyvinylphenol [6] and titanium chelates [7] are the early development of chromate-free post-sealing

solutions, but the corrosion resistance is inferior to that of chromate. SUSAC et al [8] post-treated the phosphated aluminum alloy in 4% bis-1,2-(triethoxysilyl) ethane at 25 °C, and found that the corrosion resistance of the coatings was comparable to that of chromate when the final rinse was done in a conventional chromate solution at 70 °C. YOU et al [9] found that post-sealing the phosphated galvanized steel with bis-[triethoxysilylpropyl] tetrasulfide silane can greatly improve the corrosion resistance. In the previous studies [10–12], three kinds of solutions of molybdate, cerium nitrate and silicate sol were respectively used to post-seal the phosphated galvanized steel, and the corresponding composite coatings were formed. The synergistic corrosion protection of the composite coatings plays an important role and the “with-rust” is not observed after neutral salt spray (NSS) corrosion for 5 d, where the corrosion resistance of the silicate sol post-sealed samples is better than that of the chromate post-sealed samples [10–12]. In this work, the self-healing behavior of the composite coatings obtained by phosphating and silicate sol post-sealing was examined.

**Foundation item:** Project (2012J05099) supported by the Natural Science Foundation of Fujian Province, China; Project (YKJ10021R) supported by the Scientific Research Project of Xiamen University of Technology

**Corresponding author:** Bin-lan LIN; Tel: +86-592-6291326; E-mail: linbilan@xmut.edu.cn  
DOI: 10.1016/S1003-6326(14)63403-8

## 2 Experimental

### 2.1 Preparation of coatings

The galvanized steel substrate was self-made, and the thickness of zinc layer was about 50  $\mu\text{m}$  [12]. The phosphating technologies were as follows: 1.2 g/L ZnO, 15.0 g/L NaNO<sub>3</sub>, 11 mL/L 85% H<sub>3</sub>PO<sub>4</sub>, pH of 3.0 and temperature of 45 °C [10–12]. The silicate sol post-sealing technologies were as follows: 5 g/L silicate sol, time of 10 min, temperature of 85 °C. The chemical compositions of silicate sol were 19% Na<sub>2</sub>O and 38% SiO<sub>2</sub> (mass fraction), where the molar ration of SiO<sub>2</sub> to Na<sub>2</sub>O was 2.07, thus it contained sodium silicate and SiO<sub>2</sub> sol [13]. The solutions were prepared from reagent chemicals and de-ionized water.

### 2.2 XPS analysis of chemical compositions on composite coatings

To explain the self-healing mechanism of the composite coatings more clearly, the chemical compositions on composite coatings were also studied. The composite coatings were too thin, so the signals of coatings in XRD analysis were submerged by the signals of the substrate. The element composition and valence state of the sample within 10 nm in thickness can be detected by XPS technique. In this work, XPS was used to analyze the chemical compositions of the composite coatings, where the X-ray source was Mg K<sub>α</sub>. The high resolution XPS spectra included Zn 2p, O 1s, P 2p and Si 2p.

### 2.3 SEM and EDS analysis of scratches on coated samples after NSS test

The coated samples were firstly scratched using knife with the thickness of 40  $\mu\text{m}$  and then exposed to NSS chamber for different time. The conditions of the NSS chamber were as follows: 5% NaCl solution, pH of 6.5–7.0, temperature of (35±2) °C. Finally the microstructure and chemical compositions of the scratches were investigated using SEM and EDS. And the comparison of the coated samples without scratching before and after NSS corrosion was also made.

## 3 Results and discussion

### 3.1 Chemical compositions of composite coatings

Figure 1 shows the survey and high resolution XPS spectra of the composite coatings. As shown in Fig. 1(a), there are silicon, phosphorus, oxygen, zinc and carbon on the surface of the composite coatings. However, the carbon peak disappeared after the samples were sputtered with argon ions for a few seconds. It can be considered that carbon is merely on the surface of coatings due to

the environmental contamination. In addition, the mole fractions are as follows: 34.9% O, 23.8% P, 29.7% Zn and 1.6% Si. The content of Si is high.

In Fig. 1(b), the Zn<sup>2+</sup> peak appears at the binding energy of 1022.8 eV in Zn 2p<sub>3/2</sub> spectrum which is consistent with that for Zn<sub>3</sub>(PO<sub>4</sub>)<sub>2</sub> at 1022.7 eV. In Fig. 1(c), a broad peak at 133.4 eV in the spectrum of 2p<sub>3/2</sub> is assigned to the P(+5) peak for Zn<sub>3</sub>(PO<sub>4</sub>)<sub>2</sub> at 133.4 eV.

In Fig. 1(d), the spectrum of Si 2p<sub>3/2</sub> is wide and is composed of two peaks at 102.3 eV and 103.1 eV after curve fitting. The peak of Si 2p<sub>3/2</sub> at 102.3 eV corresponds to that of ZnSiO<sub>3</sub> at 102.4 eV, and the peak at 103.1 eV is consistent with that of SiO<sub>2</sub> at 103.3 eV.

In Fig. 1(e), the wide spectrum of O 1s contains three narrow peaks with binding energy of 533.3 eV, 532.1 eV and 531.2 eV after peak fitting. The O 1s peak at 533.3 eV is consistent with that of SiO<sub>2</sub> at 533.0 eV. The O 1s peak at 532.1 eV corresponds to that of H<sub>2</sub>O at 532.2 eV. And the peak at 531.2 eV is roughly similar to that of Zn<sub>3</sub>(PO<sub>4</sub>)<sub>2</sub> at 531.5 eV and that of ZnSiO<sub>3</sub> at 531.6 eV.

It indicates that there are Zn<sub>3</sub>(PO<sub>4</sub>)<sub>2</sub>·4H<sub>2</sub>O, ZnSiO<sub>3</sub> and hydrated silica sol on the surface of the composite coatings, and silicate sol covers the phosphate coatings.

### 3.2 Microstructure and chemical compositions of scratches

The coated samples were scratched with knife until the zinc layer was exposed, and then they were corroded using NSS test. The corrosion products on the surface of the scratches after NSS corrosion for 2 h were not observed. And there were a few corrosion products on the scratches after corrosion for 4 h. After corrosion for 24 h, the corrosion products on the scratches were much. But the shape and the color of the corrosion products on the scratches were evidently different from the flocculent and loose “white-rust” on the surface of the traditional galvanized steel, as shown in Fig. 2. It should be pointed out that the “white-rust” on the traditional galvanized steel was about 35% after NSS corrosion for 2 h, and it was up to 95% after corrosion for 8 h. It shows that the corrosion rate of the exposed zinc layer on the scratches is obviously slower than that of the traditional zinc layer.

After the traditional galvanized steel was exposed in NSS atmosphere, the corrosion micro cells on the surface of zinc layer were thus formed. The corrosion process of the micro anode is the dissolution of zinc to produce Zn<sup>2+</sup>, and the micro cathode is the reduction reaction of oxygen to generate OH<sup>−</sup>. If the content of Zn<sup>2+</sup> and OH<sup>−</sup> meets the concentration product of Zn(OH)<sub>2</sub> which is  $3 \times 10^{-17}$ , Zn(OH)<sub>2</sub> is formed on the surface of zinc and subsequently dehydrated to form ZnO. With the increase

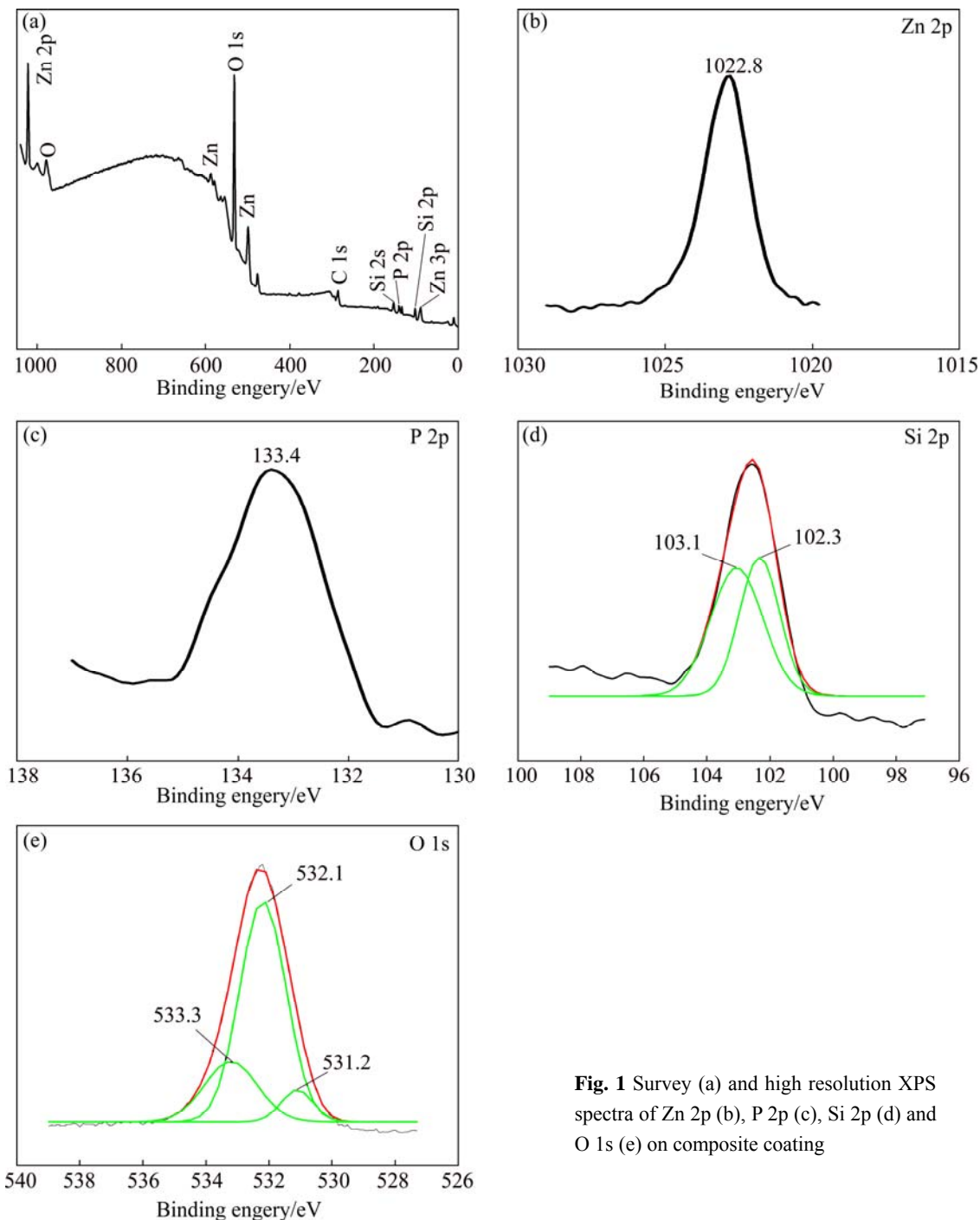


**Fig. 1** Survey (a) and high resolution XPS spectra of Zn 2p (b), P 2p (c), Si 2p (d) and O 1s (e) on composite coating

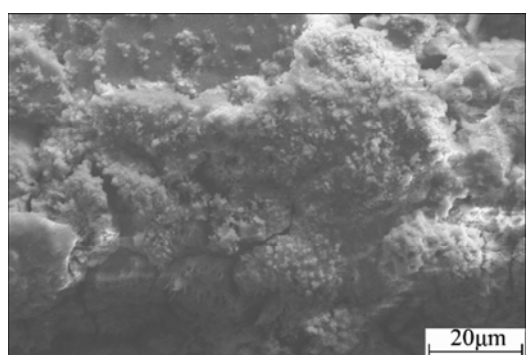


**Fig. 2** Flocculent and loose “white-rust” on galvanized steel

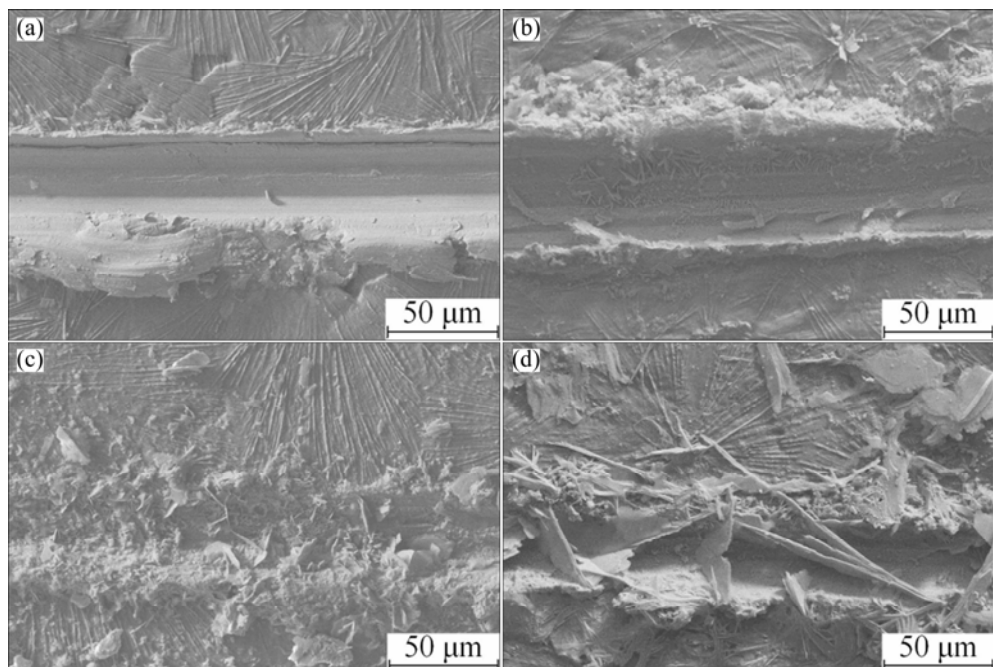
of the deposition of  $\text{Zn}(\text{OH})_2$  and  $\text{ZnO}$ , the exposed zinc layer is decreased, and the corresponding electrochemical reaction and contents of  $\text{Zn}^{2+}$  and  $\text{OH}^-$  are decreased. So the formation rate of  $\text{Zn}(\text{OH})_2$  and  $\text{ZnO}$  is also reduced. On the other hand, the competitive adsorption of  $\text{Cl}^-$  and  $\text{OH}^-$  on the surface of zinc layer takes place, which reduces the formation of  $\text{Zn}(\text{OH})_2$  and  $\text{ZnO}$ . And  $\text{Cl}^-$  also combines with  $\text{Zn}(\text{OH})_2$  to form the loose  $\text{Zn}-\text{Cl}-\text{OH}$  complex, namely basic zinc chloride (in Fig. 2). Moreover,  $\text{Cl}^-$  is the corrosion catalysis to impel the formation and the development of the pitting corrosion of zinc [14,15].

Figure 3 presents the lower magnification SEM images of the scratches on the coated samples after NSS corrosion for different time. Before corrosion, the scratch was bright and tidy, and it was the naked zinc layer, which was confirmed by the EDS analysis. The extruded coatings were on the edge of the scratch. After NSS corrosion for 2 h, there were fine acicular crystals on the scratch. When the corrosion time was increased to 12 h, the corrosion products were relatively dense and almost covered the whole scratch. After corrosion for 84 h, the corrosion products grew and a part of them passed over the scratch and continued to grow along the composite coatings. The bigger flake crystals were 50–250  $\mu\text{m}$ . Moreover, the boundary of the corrosion products and the composite coatings was exceedingly evident.

The higher magnification SEM images of the corrosion products on the scratches are shown in Fig. 4, and the corresponding chemical compositions of different micro-sites are listed in Table 1. After corrosion for 2 h, the edge and the bottom surfaces of the scratches

were fully covered with the compact, fine and needle crystals. The crystals on the edge surface were bigger than those on the bottom surface. The grain size on the edge surface was 5–10  $\mu\text{m}$ , but that on the bottom surface was smaller than 5  $\mu\text{m}$ . The crystals contain phosphorus, silicon, oxygen, zinc and chloride. And the contents of phosphorus, silicon and oxygen on the bigger crystals are larger than those on the smaller crystals. That is, there are concentration gradients of phosphorous and silicon between the bottom surface and the edge surface on the scratches. After corrosion for 12 h, the whole scratch was actually covered with the corrosion products with different sizes of crystals. The size of a part of wafer crystals were 30–50  $\mu\text{m}$ , and that of the other part of the fine and needle-like crystals was 1–5  $\mu\text{m}$ . And all the crystals contain silicon, phosphorous, oxygen, zinc and chloride.

After the scratched coated samples were placed to the NSS chamber,  $\text{Zn}_3(\text{PO}_4)_2 \cdot 4\text{H}_2\text{O}$ ,  $\text{ZnSiO}_3$  and hydrated silica sol on the composite coatings will be dissolved. All



**Fig. 3** Lower magnification SEM images of scratches on coated samples after scratching and NSS corrosion for 0 h (a), 2 h (b), 12 h (c) and 84 h (d)

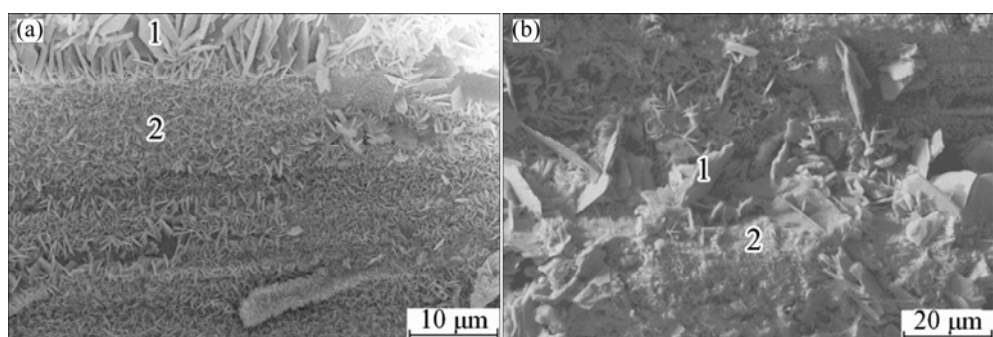


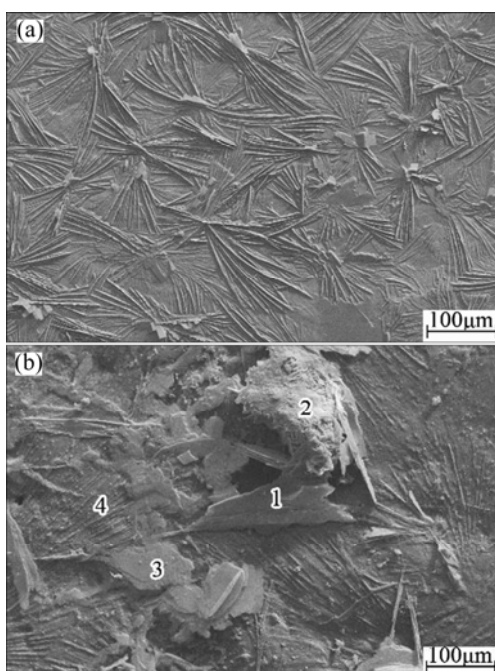
**Fig. 4** Higher magnification SEM images of scratches on coated samples after spraying for 2 h (a) and 12 h (b)

**Table 1** Element contents of different micro-sites in Fig. 4

Micro-site	Content (mass fraction)/%				
	O	Si	P	Cl	Zn
Fig. 4(a)-1	23.73	0.58	0.77	8.60	66.33
Fig. 4(a)-2	14.19	0.10	0.11	5.61	79.99
Fig. 4(b)-1	30.90	0.36	0.28	12.41	56.04
Fig. 4(b)-2	29.10	0.17	0.53	10.89	59.10

sparingly soluble compounds in aqueous medium can dissolve although the solubility is very minimal. The dissolved  $\text{PO}_4^{3-}$ ,  $\text{SiO}_3^{2-}$  and  $\text{SiO}_2$  will diffuse to the surface of the scratch and recombine with  $\text{Zn}^{2+}$  to form the insoluble compounds which cover the scratch. The concentration gradient of phosphorous and silicon on the scratches is due to the diffusion of  $\text{PO}_4^{3-}$ ,  $\text{SiO}_3^{2-}$  and  $\text{SiO}_2$  from the composite coatings to the scratch. Furthermore, the shape of the corrosion products is changed from the flocculent to the compact and fine acicular by the compounds of phosphorous and silicon, which effectively inhibits the corrosion of the exposing zinc layer. Therefore, the composite coatings obtained by phosphating and silicate sol post-sealing treatment have the ability of self-healing and  $\text{PO}_4^{3-}$ ,  $\text{SiO}_3^{2-}$  and  $\text{SiO}_2$  are the self-healing ions.

Figure 5 shows the SEM images of the composite coatings before and after NSS corrosion for 84 h, and the corresponding element contents are listed in Table 2. When the coated samples were placed in NSS chamber for 84 h, there were large wafer crystals (sites 1 and 3), fine and needle crystal groups (site 2) and the unchanged part (site 4) on the composite coatings. The unchanged

**Fig. 5** SEM images of composite coatings without corrosion (a) and after NSS corrosion for 84 h (b)**Table 2** Element contents of different micro-sites in Fig. 5

Micro-site	Content (mass fraction)/%				
	O	Si	P	Cl	Zn
Fig. 5(b)-1	24.48	0.36	0.33	13.21	61.62
Fig. 5(b)-2	31.67	0.30	0.07	13.65	54.31
Fig. 5(b)-3	26.23	0.38	0.34	12.70	60.35
Fig. 5(b)-4	23.73	3.59	4.45	5.70	62.53

part is great. All surface including needle and wafer crystals contains silicon, phosphorus, oxygen, zinc and chloride, where the content of chloride is higher and that of silicon and phosphorous is lower. It implies that in the corrosion process, the corrosion products on the defects of the composite coatings are not flocculent but needle and flake. This is in agreement with the results of the scratch experiment.

## 4 Conclusions

1) The phosphated zinc layer is post-sealed with silicate sol. Silicate and hydrated silica sol cover the pores of phosphate coatings and thus the complete composite coatings are formed.

2) The composite coatings have the self-healing ability. The amount of corrosion products on the scratches increases with increasing corrosion time and finally cover the whole scratch. And they are composed of silicon, phosphorous, oxygen, zinc and chloride.

3) During corrosion, the self-healing ions firstly dissolve from the composite coatings, and then diffuse and transfer to the scratches (defects) of the composite coatings. Subsequently, they are recombined with  $\text{Zn}^{2+}$ . Therefore, the sparkingly insoluble compounds containing silicon, phosphorous, oxygen and zinc are thus formed and cover the scratches. And the corrosion products become exceedingly compact and fine, which effectively inhibits the corrosion formation and development of the exposed zinc layer.

## References

- [1] KWIATKOWSKI L. Phosphate coatings porosity: Review of new approaches [J]. Surface Engineering, 2004, 20(4): 292–298.
- [2] ABDALLA K, RAHMAT A, AZIZAN A. Effect of copper (II) acetate pretreatment on zinc phosphate coating morphology and corrosion resistance [J]. Journal of Coatings Technology Research, 2013, 10(1): 133–139.
- [3] WANG J, ZHOU W, DU Y. Effect of sodium silicate pretreatment on phosphate layer: Morphology and corrosion resistance behavior [J]. Materials and Corrosion, 2012, 63(4): 317–22.
- [4] FOULADI M, AMADEH A. Effect of phosphating time and temperature on microstructure and corrosion behavior of magnesium phosphate coating [J]. Electrochimica Acta, 2013, 106(1): 1–12.
- [5] LIN Bi-lan, LU Jin-tang, KONG Gang. Growth and corrosion resistance of molybdate modified zinc phosphate conversion coatings

on hot-dip galvanized steel [J]. *Transactions of Nonferrous Metals Society of China*, 2007, 17(4): 755–761.

[6] LINDERT A, MAURER J I, KENT G. Chromate-free post-treatments [J]. *Products Finishing*, 1986, 50(4): 48–53.

[7] CLAFFEY W J, REID A J. Post treatment of phosphated metal surfaces by organic titanates. US 4656097 [P]. 1987-04-07

[8] SUSAC D, LEUNG C W, SUN X. Comparison of a chromic acid and a BTSE final rinse applied to phosphated 2024-T3 aluminum alloy [J]. *Surface and Coatings Technology*, 2004, 187(2–3): 216–224.

[9] YOU Wei, LU Jin-tang, LIN Bi-lan. Corrosion resistance of phosphating/silane composite film on hot-dip galvanized steel sheet [J]. *Materials Protection*, 2008, 41(3): 34–36. (in Chinese)

[10] LIN Bi-lan, LU Jin-tang, KONG Gang. Effect of molybdate post-sealing on corrosion resistance of zinc phosphate coatings on hot-dip galvanized steel [J]. *Corrosion Science*, 2008, 50(4): 962–967.

[11] LIN Bi-lan, LU Jin-tang. Effect of cerium nitrate treatment on morphology and corrosion resistance of phosphate conversion coatings [J]. *Surface Technology*, 2010, 39(4): 47–49. (in Chinese)

[12] LIN Bi-lan, LU Jin-tang, KONG Gang. Synergistic corrosion protection for galvanized steel by phosphating and sodium silicate post-sealing [J]. *Surface and Coatings Technology*, 2008, 202(9): 1831–1838.

[13] ARAMAKI K. Preparation of chromate-free, self-healing polymer films containing sodium silicate on zinc pretreated in a cerium(III) nitrate solution for preventing zinc corrosion at scratches in 0.5 M NaCl [J]. *Corrosion Science*, 2002, 44(6): 1375–1389.

[14] JEGANNATHAN S, SANKARA N T S N, RAVICHANDRAN K. Performance of zinc phosphate coatings obtained by cathodic electrochemical treatment in accelerated corrosion tests [J]. *Electrochimica Acta*, 2005, 51(2): 247–256.

[15] ARAMAKI K. XPS and EPMA studies on self-healing mechanism of a protective film composed of hydrated cerium(III) oxide and sodium phosphate on zinc [J]. *Corrosion Science*, 2003, 45(1): 199–210.

## 磷化/硅酸盐溶胶封闭后处理复合膜的自愈机理

林碧兰<sup>1</sup>, 卢锦堂<sup>2</sup>

1. 厦门理工学院 材料科学与工程学院, 厦门 361024;
2. 华南理工大学 材料科学与工程学院, 广州 510640

**摘要:** 通过磷化/硅酸盐溶胶封闭后处理技术, 在镀锌钢表面生成完整的复合膜。采用 X 射线光电子能谱研究复合膜的化学组成。将复合膜用刀片划伤至露出锌层, 经中性盐雾(NSS)腐蚀若干时间后, 采用 SEM 和 EDS 研究划痕表面腐蚀产物的显微组织和化学成分, 并与未划伤的腐蚀试样进行对比。探讨复合膜的自愈机理。结果表明, 在腐蚀过程中, 复合膜溶解出的自愈性离子扩散迁移至划痕表面或缺陷处, 与  $Zn^{2+}$ 重新结合生成不溶性化合物, 覆盖划痕或缺陷表面。腐蚀产物中含有 Si、P、O、Cl 和 Zn 五种元素, 为致密细小的针片状, 能较好阻滞裸露锌层腐蚀的形成和扩展。复合膜具有良好的自愈性能。

**关键词:** 腐蚀; 自愈性; 磷化膜; 硅酸盐; 锌

(Edited by Chao WANG)